平 成 ２ ６ 年 度

京 都 大 学 大 学 院 理 学 研 究 科

ＤＣ３回生研究発表会
要旨集

２０１５年１月２１日（水）

物 理 学 第 一 分 野

物理学第一分野ＤＣ３回生研究発表会

場所：理学研究科５号館　５階・第四講義室
発表：２０分（別に質問１０分程度）

２０１５年1月２１日（水）９：００～　開始

目　　次

１７：２０～１７：３０　休憩

Electronic Properties in heterostructures of strongly correlated electron systems

Condensed matter theory group Suguru Ueda

Abstract We investigate interface physics of various artificial heterostructures involving Mott insulators. Employing dynamical and static mean-field approximations, we uncover the presence of electronic states specific to the heterointerface. We also elucidate the spatial modulation of such phases, and shed light on correlation effects in inhomogeneous systems.

Remarkable experimental progress in fabricating atomically smooth interface allows us to access a wide range of heterostructures based on strongly correlated electron systems. Since Ohtomo *et al*. found the conducting state at the interface between insulators $LaTiO_3/SrTiO_3$ [1], many experimental and theoretical efforts have been put toward the study of their rich, complex and potentially useful behavior.

Stimulated by them, we investigate the interface physics of such correlated heterostructures involving Mott insulators with particular emphasis on the electronic/magnetic properties as well as electron correlation effects.

A fundamental issue addressed here is how electronic properties at the heterointerface differ from those of the bulk. Motivated by recent experiments on $LaTiO_3/SrTiO_3$, we first simulate the heterostructure of a Mott insulator (MI) and a band insulator (BI) [2]. The ground state phase diagram in the Hartree-Fock approximation reveals the presence of electric/magnetic ordered phases that can emerge only at the interface layer. We elucidate that these phases are derived from the strong spin/charge coupling around the interface.

It is known that the conducting interface between insulators is also observed at heterostructures of topological band-insulators (TI), whose interface (edge) state is protected by the non-trivial bulk band-structure. In order to study effects of electron correlation on such topological edge mode, we next focus on the proximity effect at the MI/TI interface employing inhomogeneous dynamical mean-field theory (DMFT) with an exact diagonalization method [3]. Our result shows that the topological edge state penetrates into the MI side, and induces strongly renormalized mid-gap states within the Mott-Hubbard gap, which are robustly stable even in the presence of the strong Coulomb interaction.

It is also demonstrated how correlation effects couple to the structure of the multilayered system. Taking an example of $LaVO_3/SrVO_3$ [4], we investigate the MI/metal superlattice structure. Our DMFT results reveal that the electrical resistivity shows a peak structure as a function of temperature, and its peak position strongly depends on the superlattice periodicity [5]. Despite its simplicity, our model provides a reasonable description for some experimental findings in the $LaVO_3/SrVO_3$ superlattice: metal-insulator transition and the temperature dependence of the resistivity.

References

[1] A. Ohtomo, D. A. Muller, J. L. Grazul, H. Y. Hwang, Nature **419**, 378 (2002).
[2] S. Ueda, N. Kawakami, and M. Sigrist, Phys. Rev. B **85**, 235112 (2012).
[3] S. Ueda, N. Kawakami, and M. Sigrist, Phys. Rev. B **87**, 161108 (2013).
[4] A. David, *et al.*, Appl. Phys. Lett. **98**, 212106 (2011).
[5] S. Ueda, N. Kawakami, (submitted).

Replica symmetry breaking in trajectories of a driven Brownian particle

Nonlinear Dynamics Group Masahiko Ueda

Abstract We study a Brownian particle passively driven by a velocity field obeying the noisy Burgers equation. We numerically and theoretically demonstrate that the system exhibits replica symmetry breaking in the path ensemble.

It has been known that equilibrium states of mean-field spin glass models freeze into some irregular patterns at low temperatures. The low temperature phase is characterized by a concept of replica symmetry breaking (RSB) [1]. RSB is a phenomenon reflecting localization of the state in a rugged free energy landscape and is detected by a physical quantity called overlap, which expresses how much two independent identical systems (replicas) are similar to each other. In RSB phase, an overlap takes a non-trivial value. These systems are one example which exhibits stable and diverse states.

In nature, there are many systems which exhibit stable and diverse dynamics. A typical example of such dynamical behavior is cell differentiation. In these systems, an observed time series is stable against perturbation like limit cycle, while a variety of trajectories are observed like chaos and Brownian motion. Behaviors of these systems are characterized by a rugged probability landscape of the trajectory. A natural question is whether there are any dynamical behaviors in which the concept of RSB in path probability appears.

Here, we present a non-equilibrium phenomenon where RSB plays an important role [2]. Concretely, we consider a passive Brownian particle driven by a random velocity field, and study whether RSB in path ensemble occurs when we focus on trajectories of the particle. As a result, we numerically find that, in case of a velocity field driven by the noisy Burgers equation [3], an overlap between two independent particles becomes non-zero. Furthermore, by changing a boundary condition of the model, we theoretically prove that the model can be mapped exactly to directed polymers in random potentials [4], which exhibit RSB. In addition, by comparing the modified system with the original system numerically, we conclude that the original system also exhibits RSB in the path ensemble. This result provides one example where the concept of RSB is useful even in non-equilibrium situation.

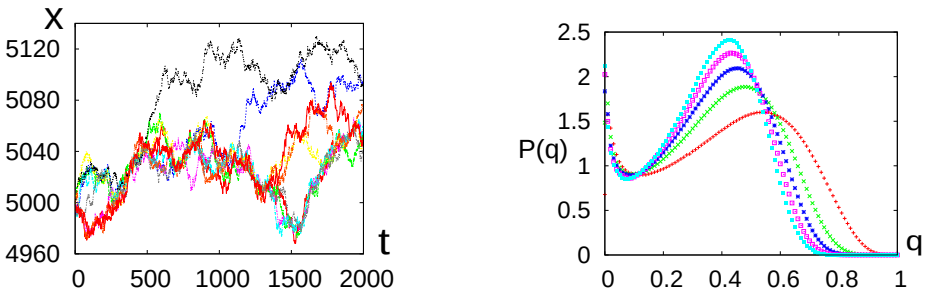

Fig. 1. (Left) Trajectories of ten Brownian particles driven by a velocity field obeying the noisy Burgers equation. (Right) Distribution of overlap for various time.

References

[1] M. Mezard, G. Parisi, and M. A. Virasoro, *Spin glass theory and beyond* (World Scientific, Singapore, 1987).
[2] M. Ueda and S.-i. Sasa, arXiv:1411.1816.
[3] M. Kardar, G. Parisi, and Y.-C. Zhang, Phys. Rev. Lett. **56**, 889 (1986).
[4] T. Halpin-Healy and Y.-C. Zhang, Physics Reports **254**, 215 (1995).

Dynamical quantum effects in cluster dynamics of Fermi systems

Condensed matter theory group, Jun'ichi Ozaki

Abstract We study cluster dynamics of Fermi systems to clarify dynamical quantum effects in those systems. We simulate collision dynamics and drag dynamics in one dimension using time-dependent density matrix renormalization group, and compare the obtained results with the semiclassical calculation. The simplified model are suggested to explain the results.

Recently non-equilibrium dynamics of cold atom systems has been enthusiastically targeted, because cold atom systems are ideal as isolated quantum systems configured in laboratory, whose parameters can be modified dynamically [1]. For example, the dynamics of quantum quench has been explored by suddenly changing the trap potential and the interaction. Also, dynamics induced by a gradual change of parameters in real time has a lot more to be investigated.

We study (i) collision dynamics of two fermion clusters and (ii) typical drag dynamics of several fermions in a fermion cloud in one-dimensional continuous systems, with particular emphasis on the non-trivial quantum many-body effects in systems whose parameters change (i) suddenly or (ii) gradually in real time. We adopt the Fermi-Hubbard model and the time-dependent density matrix renormalization group method (t-DMRG) [2] to calculate the dynamics of those systems, and we explain the simulation results by using our concise models. Finally we clarify the origin of the non-trivial quantum effects in dynamics, by comparing the results and models with semi-classical or mean-field treatments.

(i) Collision dynamics of two fermion clusters with contact interaction is simulated [3]. We calculate reflectance and transmittance of the clusters. We elucidate that the quantum effects become extremely strong with the interaction strength, leading to the transmittance much more enhanced than expected from semiclassical approximation. We propose a concise model as an application of the Bethe ansatz, which unveils the origin of the quantum effects and also explains the overall properties of the simulation results clearly. This model provides an intuitive perspective of the collision dynamics with contact interaction. Some potential applications, such as repeated collisions, are addressed.

(ii) Typical drag dynamics of several fermions in a fermion cloud in one-dimensional continuous systems is simulated [4]. We calculate the drag force on a trapped fermion cluster in a cloud of another fermion species with contact interaction. A non-trivial peak (Fig. 1) in the resistance force is observed in the high cloud density region, and it is clarified that the peak cannot be explained by a naïve mean-field theory, although the other structures are explained. This implies that some internal degrees of freedom have a crucial role in the excitation process. We also propose a criterion of effective ways in diffusive transport in a fermion cloud.

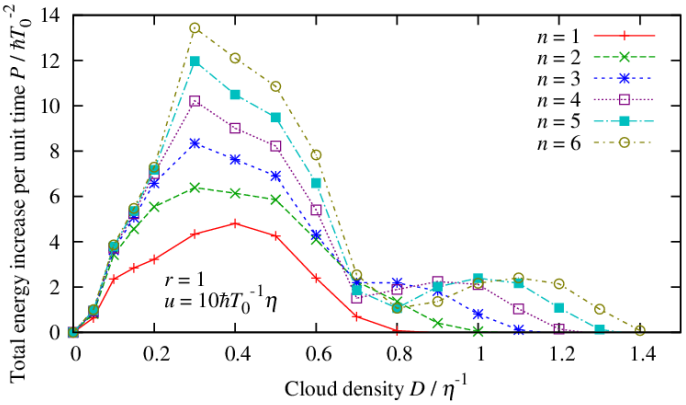

Fig. 1. Drag force versus cloud density

References

[1] A. Sommer, M. Ku, G. Roati and M.W. Zwierlein, Nature **472**, 201 (2011).
[2] S. R. White and A. E. Feiguin, Phys. Rev. Lett. **93**, 076401 (2004).
[3] J. Ozaki, M. Tezuka and N. Kawakami, Phys. Rev. A **86**, 033621 (2012).
[4] J. Ozaki, M. Tezuka and N. Kawakami, arXiv: 1402.6486.

Statistical mechanics for athermal fluctuation: Non-Gaussian noise in physics

Advanced Statistical Dynamics Lab. Kiyoshi Kanazawa

Abstract We derive Langevin-like equations with non-Gaussian noise for a wide class of athermal systems from microscopic dynamics by developing an asymptotic method. We also show that the non-Gaussian properties of the athermal noise are useful in inferring microscopic information of athermal baths. Furthermore, we derive the full-order asymptotic formula for the steady distribution function for an arbitrary non-linear friction, and show the high-order terms correspond to multiple-kicks during relaxation. As a demonstration, we study the granular motors under viscous or dry friction. Our study shows that our non-Gaussian model is the minimal model satisfying both universality and analytical simplicity.

Recently, experimental development has enabled us to investigate detailed properties of small fluctuating systems, and studies on thermal fluctuation have attracted wide interest. To understand these systems, the Langevin model has been used to describe dynamical properties of thermal fluctuation. The Langevin equation is a linear stochastic model with the Gaussian noise, and is analytically solvable. Moreover, this model can be asymptotically derived for a wide class of systems associated with single stochastic environments in the small noise limit[1], which proves the universality of this model.

On the other hand, non-Gaussian fluctuation is reported to appear for athermally fluctuating systems. A natural question would then arises: *When and how does the non-Gaussianity emerge from microscopic dynamics?* This question has not yet been fully answered. Indeed, the conventional coarse-graining theories fail to explain non-Gaussian behaviors at leading order because of the central limit theorem (CLT). In this presentation, we show an answer to this question. We asymptotically derive Langevin-like non-Gaussian models for a wide class of stochastic systems associated with thermal and athermal baths under three assumptions: (i)large system size, (ii)strong thermal friction, (iii)coexistence of the thermal and athermal noise[2, 3]. We also show that the non-Gaussian properties of the athermal fluctuation can be used to infer microscopic information of the athermal bath. Furthermore, we show the full-order asymptotic formula for the steady distribution for an arbitrary non-linear friction, and illustrate that the high-order terms directly correspond to multiple-kicks processes during relaxation by introducing a diagrammatic representation[3]. As a demonstration, we study granular motors under viscous or dry friction, and verify our formulation numerically. Our study shows that the non-Gaussian Langevin equation is the minimal model satisfying both physical universality and analytical simplicity.

References

[1] N.G. van Kampen, Stochastic Processes in Physics and Chemistry, North-Holland (2007).
[2] K. Kanazawa, T.G. Sano, T. Sagawa, and H. Hayakawa, arXiv: 1407.5267 (2014).
[3] K. Kanazawa, T.G. Sano, T. Sagawa, and H. Hayakawa, arXiv: 1412.2233 (2014).

Classical Reduction of Quantum Master Equations as Similarity Transformation

Non-equilibrium Physics Group　　Norikazu Kamiya

Abstract We investigate classical reduction of quantum master equations by similarity transformation of the Liouvillian. The method is applied to quantum energy transport and the transport efficiency problem.

The quantum master equation approach is a standard tool in studies of quantum open systems. In their analysis, the rotating wave approximation (RWA) is commonly used on the quantum master equation to obtain the Lindblad equation, which ensures the trace-preserving property and complete positivity. In the RWA, the diagonal and off-diagonal elements of the density matrix in the energy representation are split, resulting in the diagonal stationary solution. However, internal energy currents are off-diagonal in the energy basis. Consequently, there is no resulting energy flow for the RWA master equation [1].

The RWA can be regarded as classical reduction of the quantum master equation. These classical reductions are formally described by the projection operator technique. However, the projection operator technique does not give a solution of the problem of energy currents in the RWA.

In this work, we present a new formulation of quantum-to-classical reduction of quantum master equations utilizing a similarity transformation of the Liouvillian [2]. Our formulation reveals the necessity of the transformation of observables, which gives a solution of the problem in the RWA scheme. We discuss the transformation of an energy current using a certain simple example.

Moreover, we show that the quantum master equation can be exactly replaced with classical master equation for the calculation of a quantity such as quantum transport efficiency. We discuss the single exciton on a tight binding Hamiltonian with dissipation. The transport efficiency is defined as how often the particle trapped at the trapping site. We confirm the exact quantum-to-classical replacement by the numerical calculation (Fig. 1).

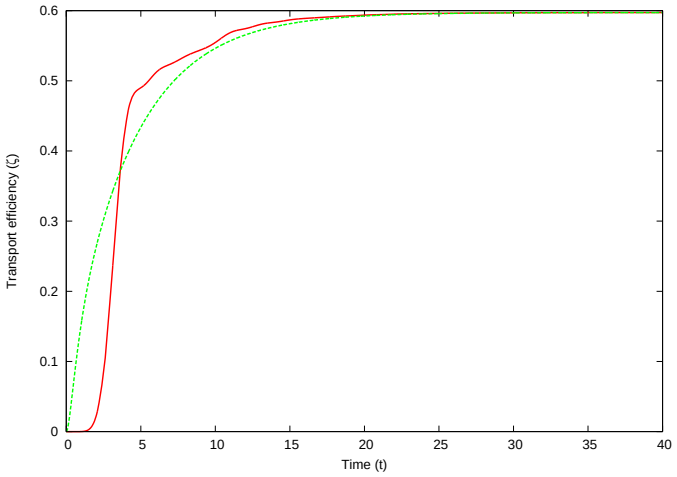

Fig. 1: Transport efficiency as a function of time. Dashed line denotes the quantum dynamics and solid-line denotes the replaced classical dynamics.

References

[1] H. Wichterich, M. J. Henrich, H-P. Breuer, J. Gemmer, and M. Michel, Phys. Rev. E **76**, 031115 (2007)
[2] N. Kamiya, submitted.

Ferromagnetic critical behavior and critical universality in itinerant-electron metamagnet UCoAl

Quantum Materials Lab. Kosuke KARUBE

Abstract In order to investigate static and dynamic properties around a critical endpoint (CEP) and a tricritical point (TCP) in itinerant ferromagnetic systems, we have performed nuclear magnetic resonance and nuclear quadrupole resonance measurements for an itinerant metamagnet UCoAl. We observed the development of magnetic fluctuations near the CEP and TCP.

Itinerant-electron ferromagnetic (FM) materials are expected to follow an universal 3D (temperature - magnetic field - pressure) phase diagram characterized by the presence of a tricritical point (TCP), where a FM transition changes from second-order to first-order, and a critical endpoint (CEP), where a first-order field-induced FM transition [metamagnetic (MM) transition] changes to a crossover[1]. We focused on an itinerant metamagnet UCoAl as a suitable material to clarify the static and dynamic magnetic properties around these critical points since it shows a MM transition at low fields. We have performed ^{27}Al- and ^{59}Co-nuclear magnetic resonance (NMR) and nuclear quadrupole resonance (NQR) measurements in order to estimate the *c*-axis magnetization (M_c) (order parameter) and the *c*-axis magnetic fluctuations (S_c) under the precise control of tuning parameters: temperature (T), magnetic field along the *c*-axis (H_c), uniaxial pressure along the *b*- and *c*-axes ($P_{||b,c}$), and substituted Fe concentration (x).

At ambient pressure, we observed the Ising-type anisotropy along the *c*-axis in both magnetization and magnetic fluctuations. In addition, S_c exhibits a broad maximum at T_{max} ~ 20 K even in H_c = 0, which is a characteristic feature in itinerant metamagnets. The contour plots of M_c and S_c on the T - H_c phase diagram at ambient pressure show the presence of the CEP at (T, $\mu_0 H_c$) ~ (12 K, 1.0 T) and the divergence of S_c at the CEP as shown in Fig. 1. From the estimation of critical exponents around the CEP, we found that the MM critical behaviors in UCoAl are categorized into a 3D-Ising universality class as observed in the gas-liquid and 3D-Mott transitions[2]. Uniaxial pressure $P_{||b}$ and $P_{||c}$ give rise to the opposite magnetic response; $P_{||b}$ suppresses the FM state, whereas, $P_{||c}$ induces the FM state even in H_c = 0. Furthermore, the peak intensity of S_c at T_{max} ~ 20 K in H_c = 0 is suppressed by $P_{||b}$, whereas, it is enhanced by $P_{||c}$ and maximized around (T, $P_{||c}$) ~ (20 K, 0.16 GPa), indicating that FM fluctuations are enhanced toward the TCP[3]. Fe-substituted U(Co$_{1-x}$Fe$_x$)Al clearly shows the first-order FM transition in H_c = 0 in the x range of 1-2%. The first-order FM transition line and T_{max} line seem to merge around (T, x) ~ (20 K, 2.5%), which suggests the presence of the TCP as theoretically predicted. Taking the above $P_{||c}$ measurement into consideration, S_c at T_{max} ~ 20 K develops with approaching the TCP.

In conclusion, we have confirmed the presence of the universal 3D phase diagram in UCoAl and revealed the development of FM critical fluctuations at the CEP and TCP.

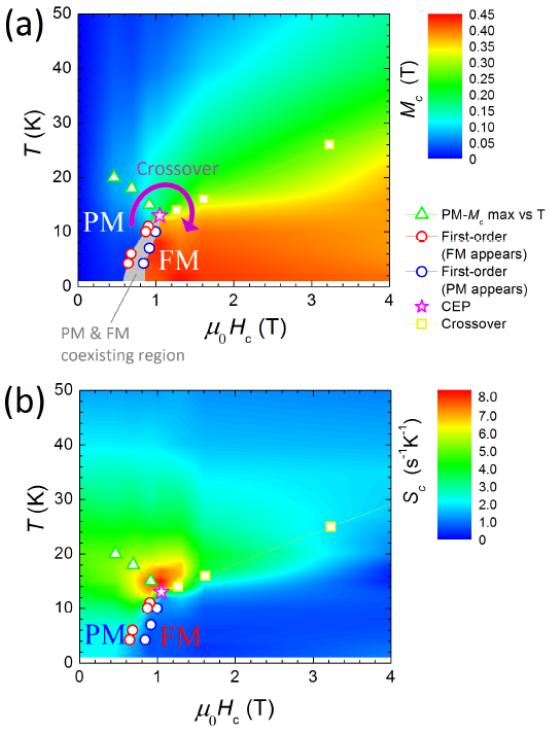

Fig. 1. Contour plots of (a) *c*-axis magnetization (M_c) and (b) *c*-axis magnetic fluctuations (S_c) on the T - H_c phase diagram at ambient pressure in UCoAl.

References

[1] D. Belitz *et al.*, Phys. Rev. Lett. **94**, 247205 (2005).
[2] K. Karube *et al.*, Phys. Rev. B **86**, 024428 (2012).
[3] K. Karube *et al.*, J. Phys. Soc. Jpn. **83**, 084706 (2014).

Inelastic X-ray Scattering Study of Plasmons in Liquid Alkali Metals

Physics of Disordered Systems Group Koji Kimura

Abstract We investigate plasmons in liquid alkali metals using inelastic x-ray scattering (IXS) techniques. Variations in the plasmon behaviors upon melting, observed in the IXS experiments, are discussed in terms of structural disorder in liquid metals. In particular, the change in the line width is reproduced by a newly derived formula.

The electronic states in liquid metals are less clearly understood than in crystalline systems, because of the disordered structure in the liquid state. Several properties of liquid metals, such as optical reflectivity [1] and electronic excitations [2], have not been sufficiently studied in relation to the disordered structure. In fact, effects of ions on these properties in liquid metals have been discussed only based on the similarity of the local structure in the liquid state to that in the solid state, and influences of the structural disorder have not been clarified adequately.

Behaviors of plasmon, a collective excitation of electrons, reflect the electron-ion interaction. Thus we can investigate the influence of the ions on the electronic excitations in liquid metals, through the plasmons.

In this work, we performed inelastic x-ray scattering (IXS) experiments for solid and liquid Rb to clarify the effect of structural disorder on plasmon behaviors in liquid metals [3]. We observed inelastic peaks arising from plasmons in the IXS spectra for solid and liquid Rb. From the IXS spectra, we determined the plasmon excitation energy ($\hbar\omega_{\mathrm{p}}$) and the line width ($\Delta E_{1/2}$) as a function of the momentum transfer q.

Figure 1 (a) shows $\hbar\omega_{\mathrm{p}}(q)$ of solid and liquid Rb. As seen in the figure, $\hbar\omega_{\mathrm{p}}(q)$ of liquid Rb tends to increase with q, while that of solid Rb shows cusp-like shape, where $\hbar\omega_{\mathrm{p}}(q)$ increases in q < 0.5 Å^{-1} and decreases in q > 0.6 Å^{-1} with increasing q. Figure 1 (b) shows $\Delta E_{1/2}(q)$ of solid and liquid Rb. We can see that $\Delta E_{1/2}(q)$ of liquid Rb tends to be narrower than that of solid Rb for q < 0.5 Å^{-1}. This tendency is more clearly seen in the inset of Fig. 1 (b), which shows the difference of $\Delta E_{1/2}(q)$ between solid and liquid Rb. The variations in $\hbar\omega_{\mathrm{p}}(q)$ and $\Delta E_{1/2}(q)$ upon melting are discussed in terms of the difference of the ionic structures between solid Rb and liquid Rb, and it is suggested that the effect of the ionic potential on the plasmon behavior in liquid Rb is weaker than that in solid Rb. In particular, we have newly derived a formula for evaluating $\Delta E_{1/2}(q)$ in liquid metals at q = 0 [4], where disordered structure in the liquid state is taken into account, and reproduced the experimentally observed narrowing of the line width.

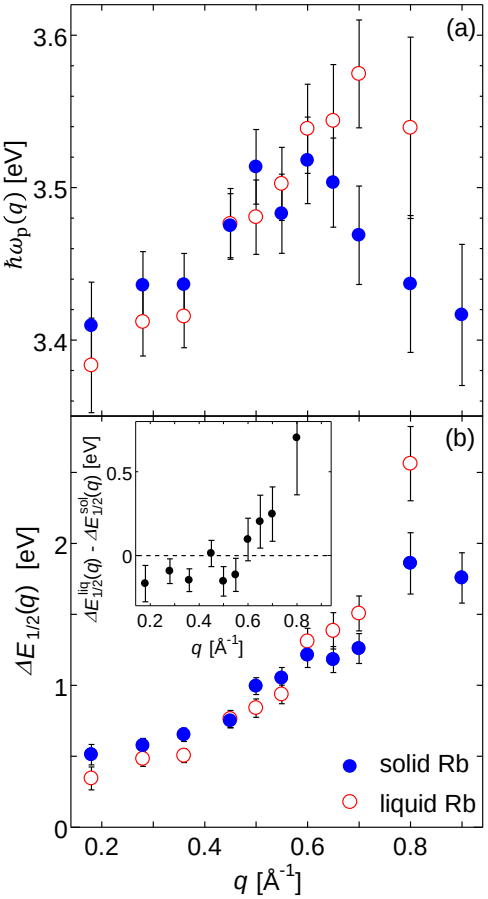

Fig. 1. (a) Plasmon excitation energy, $\hbar\omega_{\mathrm{p}}$, and (b) the line width, $\Delta E_{1/2}$, in solid and liquid Rb as a function of q. The inset shows the difference of $\Delta E_{1/2}$ between solid and liquid Rb, $\Delta E^{\mathrm{liq}}_{1/2}(q) - \Delta E^{\mathrm{sol}}_{1/2}(q)$.

References

[1] B. Knuth, F. Hensel, and W. W. Warren Jr, J. Phys.: Condens. Matter **9** 2693 (1997).
[2] J. P. Hill, C. C. Kao, W. A. C. Caliebe, D. Gibbs, B. Hastings, Phys. Rev. Lett. **77**, 3665 (1996).
[3] K. Kimura, K. Matsuda, N. Hiraoka, *et al.*, Phys. Rev. B **89**, 014206 (2014).
[4] K. Kimura, K. Matsuda, and M. Yao, J. Phys. Soc. Jpn. **82**, 115001 (2013).

Topological crystalline phases with order-two point group symmetry

Condensed matter theory group Ken Shiozaki

Abstract We present the complete classification of topological crystalline insulators and superconductors with order-two point group symmetry by using *K*-theory. The obtained classification shows that defect gapless states can be considered as boundary states, and a novel realization of the bulk-boundary correspondence in terms of *K*-theory.

In this decade, topological phases have provided a new area of study in condensed matter physics. Topological insulators and superconductors are classes of topological phases of free fermions. The bulk materials are described by the non-interacting single particle Hamiltonians. The bulk shows no low-energy excitation because of a finite excitation gap, thus, all physically observable phenomena can occur at their boundaries or topological defects. The topological nontriviality of the bulk reflects an existence of robust gapless excitations at the boundaries or their defects. Topological phases are classified according to symmetries such as the time-reversal symmetry and the particle-hole symmetry. Space group symmetries originating from crystalline structures also give finer classifications of topological phases, which enable some trivial phases without crystalline symmetries to be topologically nontrivial phases. It is naively expected that the gapless boundary modes in topological crystalline insulators and superconductors are fragile against disorders because these specific symmetries are microscopically sensitive to small disorder effect. But recent studies of topological crystalline insulators have shown that if the symmetries are preserved on average, then for some symmetry classes the existence of gapless boundary states is rather robust. Moreover, surface gapless states protected by the mirror reflection symmetry have been observed experimentally. Such recent developments motivate us to classify topological crystalline insulators and superconductors, and reveal their unified low-energy physics. Some topological crystalline phases with simple point group symmetries have been classified. However, there is no knowledge of an algorithmic method of the classification of topological crystalline phases for general space group symmetries.

For order-two point group and magnetic point group symmetries, we can successfully classify all the topological phases of free fermions by using the Clifford algebras and *K*-theory. The order-two point group symmetries we consider are general and include Z_2 global spin flip, reflection, twofold rotation, inversion, and their magnetic symmetries. An additional order-two symmetry provides a new generator of the Clifford algebra and shifts classifying spaces of Hamiltonians. We can construct various *K*-group isomorphisms between different space dimensions and symmetries, leading to the complete classification of the topological crystalline phases with order-two point group symmetries. Various symmetry protected topological phases and gapless modes will be identified and discussed in a unified framework. Obtained topological classification suggests that defect gapless excitations can be considered as boundary states of lower-dimensional crystalline insulators and superconductors. We also present topological classification of symmetry protected Fermi points. The bulk classification and the surface Fermi point classification provide a novel realization of the bulk-boundary correspondence in terms of *K*-theory.

Reference

Ken Shiozaki and Masatoshi Sato, Phys. Rev. B **90**, 165114 (2014).

Theoretical Study of Electron Dynamics in Multi-Orbital Antiferromagnetic Metals

Physics of Matter: Condensed Matter Physics (YITP) Koudai Sugimoto

Abstract In order to understand the multi-orbital physics in antiferromagnetic phase, we investigate iron arsenide and chromium. We elucidate the origin of in-plane anisotropic resistivity in iron arsenide with a memory-function approach, and calculate resonant inelastic x-ray scattering spectra in chromium.

Chromium (Cr) is known to be a typical antiferromagnetic metal characterized by an incommensurate spin-density-wave (SDW) ground state due to the Fermi-surface nesting. The magnetic and electronic properties of Cr have widely been investigated for a long time. Such studies of 3*d* transition-metal compounds have been renewed by a recent discovery of iron-based superconductors, and newly focused on the aspect of the multi-orbital nature of 3*d* atoms. In the field of iron-based superconductors, it is now recognized that the orbital degrees of freedom play a crucial role not only in the mechanism of superconductivity but also in the understanding of antiferromagnetic metallic phase adjacent to the superconducting phase. Therefore, it is important to include all of $3d$ orbitals in theoretical works of transition-metal compounds. Physical properties of the typical transition-metal compound, chromium, must be accordingly reinvestigated from this viewpoint. In this thesis, we theoretically study the electron dynamics in multi-orbital antiferromagnetic metals, especially focusing on iron arsenide and Cr. Our aim of studying both materials is to deepen our understanding of the physics of antiferromagnetic transition-metal compounds characterized by multi-orbital nature.

The parent compound of iron-arsenide superconductors exhibits an antiferromagnetism with stripe-type order below Neel temperature. The band structure of the stripe phase is characterized by Dirac-type dispersions, which are induced by the folded paramagnetic dispersion with multi-orbital nature. In the stripe phase, the resistivity shows anisotropy in the conducting Fe-As plane. The experimental data suggest that impurities play a crucial role in the anisotropy. We start with a five-3*d*-orbital Hubbard model, and use a mean-field approximation. Then, we examine the anisotropy of resistivity by applying the memory-function approach treating isotropic nonmagnetic impurities. The resistivity obtained by the memory-function approach yields a proper anisotropic behavior near the undoped region: The resistivity in the antiferromagnetically ordered direction is first smaller than that in the ferromagnetically ordered direction, and the anisotropy reverses as holes are introduced. The origin of the anisotropy can be understood from the interplay of impurity scattering and the character of Fermi surfaces including the Dirac-type one [1].

Motivated by the crucial role of orbitals in the iron-arsenide antiferromagnetic metallic phase, we reinvestigate electron dynamics of the typical itinerant SDW metal, Cr [2]. We again use multi-band Hubbard model composed of 3*d* and 4*s* orbitals. After the SDW mean-field approximation, we obtain the dynamical spin susceptibilities and L_3-edge resonant inelastic x-ray scattering (RIXS) spectra by employing random phase approximation. In our calculation, we assume the perfect commensurate SDW state. We find a collective spin-wave excitation undamped up to ~0.6 eV. Above the energy, excitations overlap individual particle-hole excitations as expected. In RIXS spectra, particle-hole excitations with various orbital channels show a large spectral weight, masking the spectra of the spin collective mode. However, it may be possible to detect the spin-wave excitation in RIXS experiments in the future if resolution is high enough.

The above two topics in this thesis provide the evidence of crucial roles of 3*d* orbitals in the antiferromagntic metal of 3*d* transition-metal compounds. This contributes to the deeper understanding of the physics of multi-orbital antiferromagnetic metal.

References

[1] K. Sugimoto, P. Prelovšek, E. Kaneshita, and T. Tohyama, Phys. Rev. B **90**, 125157 (2014).
[2] K. Sugimoto, Z. Li, E. Kaneshita, K. Tsutsui, and T. Tohyama, Phys. Rev. B **87**, 134418 (2013).

Numerical simulation of two-frequency forced Faraday waves with level-set method

Fluid Physics Group Kentaro Takagi

Abstract We performed a numerical simulation of two-frequency forced Faraday waves with level-set method. The pattern observed only in two-frequency forced Faraday waves was numerically reproduced for the first time. Our numerical results show that assumption of a weakly nonlinear analysis of the pattern is incomplete.

Faraday waves are standing waves forming a fascinating pattern in the fluid interface subjected to typical vertical periodic force. Although Faraday waves were found two hundred years ago, many researchers have been attracted even today since new nonlinear phenomena continue to be found. For example, there are two-frequency forced Faraday waves. In some experiments [1], more complex patterns than the single frequency case are reported. The linear stability analysis [2] and the weakly nonlinear analysis [3] are applied to two-frequency Faraday waves were developed. While a number of patterns of two-frequency forced Faraday waves can be described by these analyses, some essential but complex patterns have not been understood. Therefore, three dimensional numerical simulation is required to elucidate the mechanism. In this study, we performed the first numerical simulation of two-frequency forced Faraday waves.

Périnet *et al.* [4] performed the first three dimensional numerical simulation of Faraday waves with single frequency vibration. Their results are consistent with those of laboratory experiments quantitatively. However, their numerical scheme is not suitable for recent complex Faraday waves, because their implementation can not describe complex interfaces with large deformation. Since we aim to reproduce not only two-frequency forced Faraday waves, but also other complex patterns, we adopt an interface tracking scheme method called level-set method different from Périent *et al.*

In order to validate our three dimensional simulation scheme, the results were compared with those of the linear stability analysis [2]. As shown in Fig. 1, our results are consistent with those of the linear stability analysis quantitatively. Moreover, for the validation in a nonlinear regime, we reproduced square and hexagon patterns with identical physical properties to the experiment [1]. After these validations, we succeeded in reproducing the rhomboidal pattern for the first time. This pattern is observed only in two-frequency forced Faraday waves. The interface profile is shown in Fig. 2.

Finally, we check whether the assumptions made in the weakly nonlinear analysis for the rhomboidal pattern [3] are reasonable by comparing with our simulation results. It is assumed that a damping parameter are small and the amplitudes vary slowly. However, our numerical results show that the assumptions are not reasonable. Consequently, the weakly nonlinear analysis of the rhomboidal pattern is incomplete and has to be improved.

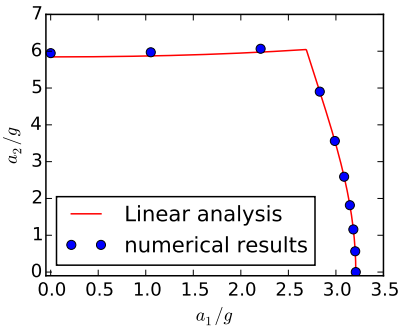

Fig.1 Comparison of numerical results with linear stability analysis. The x and y axes represent the normalized vibration amplitudes.

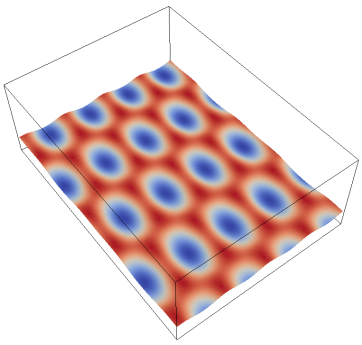

Fig.2 The surface profile of rhomboidal patterns colored by its interface height.

References

[1] H.Arbell and J.Fineberg, Phys. Rev. Lett. **85**:756–759 (2000).
[2] T.Besson, W.Edwards and L.Tuckerman Phys. Rev. E **54**:507–513 (1996).
[3] J.Porter and M.Silber, Phys. Rev. Lett. **89**:084501 (2002).
[4] N.Périnet, D.Juric and L.Tuckerman J. Fluid Mech. **635**:1 (2009).

Correlation effects on a two-dimensional topological insulator

Condensed matter theory group Yuto Takenaka

Abstract We address the effect of Coulomb interactions in topological band insulators. In order to study how interactions affect the topological properties, we apply the variational Monte Carlo method to the two-dimensional topological model.

Recently, the topological band insulator (TBI) has been one of the current important issues in condensed matter physics. In TBI, spin-orbit coupling leads to a time-reversal invariant band structure with a full insulating gap in the bulk and gapless edge states on the boundaries. While the essential features of the TBI can be described as a one-body problem, the electron correlation effects are expected to create novel topological states. For example, iridium compounds, such as Na_2IrO_3 and $A_2Ir_2O_7$ (A=Pr, Eu) have recently been proposed as materials in which the interplay of spin-orbit coupling and electron interaction effects might be important [1, 2].

Many theoretical analyses of electron correlation effects in TBIs are calculated by mean field theory, such as dynamical mean field theory (DMFT) or slave-boson mean field theory (SVMF) in the periodic boundary condition [2, 3]. In order to study how electron interactions affect the edge states and bulk states respectively, it is important to consider spatial dependence due to the lack of translational symmetry perpendicular to the boundaries in finite dimensions.

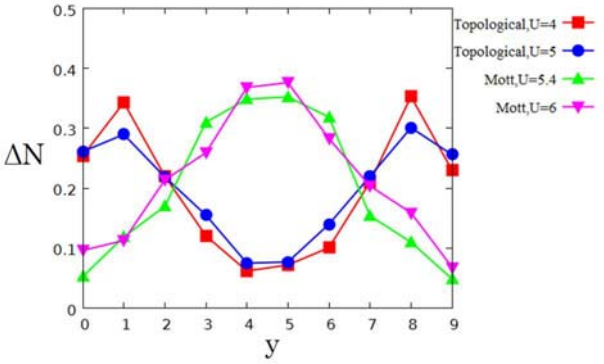

Fig. 1. U-dependence of the electron distribution

In this study, we investigate a generalized Bernevig-Hughes-Zhang model [4] having electron correlations with the variational Monte Carlo (VMC) method. With this method, we can accurately estimate the ground-state properties. In order to study spatial dependence of Coulomb interactions, we consider the periodic (open) boundary condition in x- (y-) direction and introduce spatially-dependent (y-dependent) variational parameters.

We calculate the ground-state energy and the double occupancy. From these data, we show that a first-order transition occurs in this model, which is accompanied by the coexistence region by the hysteresis. In order to clarify the topological properties, we consider the electron distribution. We show that the qualitative behavior of the electron distribution clearly changes around the Mott transition point, and edge states disappear (Fig.1). In order to discuss how the correlations affect electronic properties in the TBI, we also calculate the spin and charge structure factors. Comparing these data with previous studies, we discuss the effect of Coulomb interactions in the TBIs.

References

[1] A. Shitade, *et al*, Phys. Rev. Lett. **102**, 256403 (2009)
[2] D. A. Pesin and L. Balents, Nat. Phys. **6**, 376 (2010)
[3] T. Yoshida, S. Fujimoto, and N. Kawakami, Phys. Rev. B **85**, 125113 (2012)
[4] B. A. Bernevig, T. L. Hughes and S. C. Zhang, Science, **314**, 1757 (2006)

Two types of spinning motion of active deformable particles

Nonlinear Dynamics Group Mitsusuke Tarama

Abstract: Two types of spinning motions of active deformable particles are investigated theoretically. One is the spinning motion due to the rotation of the whole body. Besides, shape deformation may travel along the interface, which is regarded as another type of spinning motion in terms of the particle dynamics.

Active matter, or active particle, is an object that converts potential energy into kinetic energy in itself and consequently undergoes systematic movements. Major realisations of active matter are found in colloidal systems such as Janus colloids, where one side of the surface is functionalised to have a difference in, for instance, the chemical property from the other. Colloidal active particles are usually rigid, but there are also deformable active particles like liquid droplets that undergo chemical reactions on the interface, which is soft and does change its shape during its spontaneous movement. Indeed, deformability is of basic importance for most of the biological processes. Dynamics of such active deformable particles are actually what we are interested in here.

Active motions, which are the motions that active particles exhibit spontaneously, include not only a translational motion of the centre of mass, but also a spinning motion, i.e. the rotation around the centre of mass, deformations of the shape, a self-replication, and a fusion of active particles. In this presentation, we concentrate ourselves on the spinning motion of active deformable particles. We propose the argument that there are at least two types of spinning motion for active deformable particles. On the one hand, an active particle undergoes a spinning motion due to the rotation of a whole body (*type-I spinning motion*). This type of spinning motion corresponds to that of a classical rigid body. On the other hand, when the particle is soft and hence does change its shape, the deformation of the particle shape may travel along the interface. In terms of the dynamics of the particle, this traveling wave of shape deformation is regarded as a spinning motion (*type-II spinning motion*).

In order to confirm this proposition, we demonstrated the dynamics of active deformable particles by introducing model equations for each spinning motion. We described the rotation of the particle by an antisymmetric tensor variable, and the shape deformation by using symmetric deformation tensors. To keep the argument simple and general, we derived nonlinearly coupled time-evolution equations for these variables as well as the velocity of the centre of mass from symmetry considerations, which therefore do not depend on any specific mechanisms. First, we showed that the type-I spinning motion appears when the antisymmetric tensor representing the rotation of the particle takes a non-vanishing value by breaking the symmetry spontaneously [1,2,4]. In contrast, we analytically predicted and verified numerically [3] that the coupled equations of motion for the quadratic and quartic deformations experience instability in the angular direction for finite magnitude of deformations, and thus the deformations starts to travel along the interface. This traveling wave of deformations is regarded as a spinning motion concerning the dynamics of the particle. Since this spinning motion appears independently of the rotational variable of the particle and instead the traveling wave of deformations plays an important role, we may conclude it is a different dynamical mode from the type-I spinning motion and indeed it is the type-II spinning motion. In this case, an oscillatory motion of the shape deformation was also obtained. We address that the model for the type-II spinning motion is further generalised to the coupled equations of nth- and $2n$th-mode deformations, which possess mathematical symmetry for different n. Each of these two types of spinning motion has been observed experimentally. Moreover, a cell that exhibits the type-II spinning motion was found to experience an oscillation of the deformation as well.

References

[1] M. Tarama and T. Ohta, J. Phys.: Condens. Matter **24**, 464129 (2012).
[2] M. Tarama and T. Ohta, Prog. Theor. Exp. Phys. **2013**, 013A01 (2013).
[3] M. Tarama and T. Ohta, Phys. Rev. E **87**, 062912 (2013).
[4] M. Tarama, Y. Itino, A.M. Menzel, and T. Ohta, Eur. Phys. J. Special Topics **223**, 121–139 (2014).

Phenomenological structure for large deviation principle in time-series statistics

Nonlinear Dynamics Group　　Takahiro Nemoto

Abstract We propose a calculation method of the large deviation functions of time-averaged quantities based on the idea for measuring thermodynamic functions. We then apply our method to non-equilibrium lattice gasses and study the effective descriptions of the exponentially biased ensembles in them.

Thermodynamic functions provide quantitative relations among macroscopic observables in equilibrium systems. These functions are constructed by operational (or phenomenological) manners within the theory of thermodynamics. On the other side, from the statistical mechanics, which connects the thermodynamic functions to microscopic theories such as Newtonian dynamics, one has known that the thermodynamic functions also play a role of the large deviation functions of thermodynamic variables. This structure is suggestive, and recently, several results, for extending this structure to the large deviation functions of time-averaged quantities in non-equilibrium systems, have been developed.

In time-series statistics, the large deviation functions are connected to the frequency of rare events. Then, what follows from the phenomenology similar to thermodynamics for constructing these large deviation functions within an operational manner, if it exists? On one hand, the large deviation functions are phenomenologically obtained. On the other hand, it describes the frequency of rare events characterized by large deviation principle. Such a phenomenology should become a rare event sampling method that can be used in real experiments. In this talk, I am going to propose a computational method of large deviation functions of time-averaged quantity [1], which is based on this idea.

We apply the proposed method to numerical studies of non-equilibrium lattice gases, which are an ASEP (Asymmetric Simple Exclusion Process) and a KCM (Kinetically constrained model). Both of them are many-body systems and several non-trivial results have been found in the previous studies of them. We calculate the cumulant generating functions (or large deviation functions) of time-averaged quantities in these models, from which we study the dominant interactions in those models, when rare events are taking place (Fig.1).

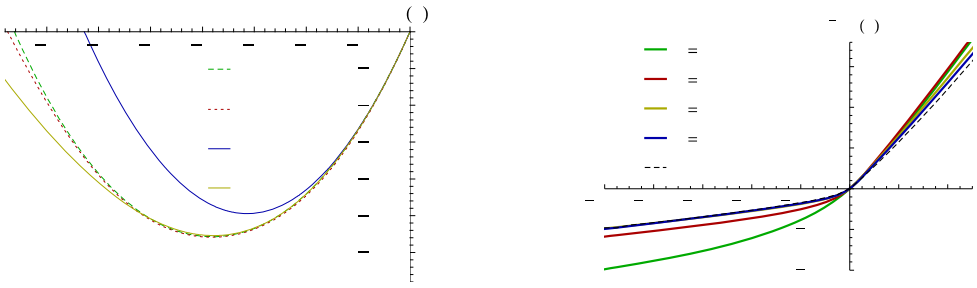

Fig. 1. Cumulant generating functions of non-equilibrium lattice gasses. By combining our method with truncated transition rates, we investigate which interactions are important in rare events. The left figure is for ASEP with a one-body-potential approximation, and the right figure is for a KCM with a short-range-interaction approximation.

References

[1] T. Nemoto and S. Sasa, Phys. Rev. Lett. 112, 090602 (2014).

Excitonic finestructure and nonequilibrium phase transition of the electron-hole system in diamond

Solid-state spectroscopy group　Yuji Hazama

Abstract We investigate nonequilibrium phase transition of the electron-hole system in diamond. We elucidate the origin of the fine structure of excitons and observe a signature of a continuous transition below the critical temperature. We find that the unconventional phase transition is caused by dissipation of carriers due to the recombination.

Photoexcited electron-hole systems in semiconductors have long been investigated because they are suited to the study of nonequilibrium many-body physics. It is well known that the introduction of valley degrees of freedom in indirect-gap semiconductors drastically changes macroscopic behaviors of the system. For example, few-body bound states of electron-hole pairs (polyexcitons) are considered to be stabilized [1] in silicon. It was also expected that polyexcitons would strongly affect the gas-liquid phase transition between the exciton and the electron-hole liquid (EHL). However, the relation between valley degrees of freedom and the stability of polyexcitons is unexplored because the small binding energies of polyexcitons in silicon hinder detailed spectroscopic measurements. The influence of polyexcitons on the phase transition is also unknown because we need to access temperatures sufficiently lower than the critical temperature of EHL though it is impossible for silicon by using standard cryogenic techniques.

In order to overcome such difficulties, we focused on diamond whose polyexcitons' binding energies and critical temperature are extremely high: a few tens of meV [2] and 165 K [3], respectively. We first investigated the origin of the fine structure of excitons by high-resolution spectroscopy, and found that the fine structure occurs due to the competition between three effects: the spin-orbit interaction of the hole, the exchange interaction between the electron and the hole, and the effective mass anisotropy of the electron. Second, we proposed and demonstrated a photoexcitation method by which the effective temperature of excitons can be kept as low as 15 K up to the density of 10^{19} cm^{-3}. Finally, we performed photoluminescence spectroscopy at various temperatures and densities using our new excitation method. We observed polyexcitons below 30 K while thermodynamic theory predicts that EHL is more stabilized than polyexcitons. We also found that the gas-liquid phase transition below 25 K shows the signature of a continuous phase transition while a gas-liquid phase transition below critical temperature is of first-order in general (see Fig. 1). We revealed that the unprecedented transition is caused by the nonequilibrium nature of the electron-hole system originating from dissipation of carriers due to the recombination.

Our findings are important in two senses. First, the origin of the excitonic fine structure will benefit the investigation of the internal structure of polyexcitons. Second, our result on the nonequilibrium gas-liquid phase transition indicated that dissipation can drastically change thermodynamic properties of a system even for the most elementary phase transition.

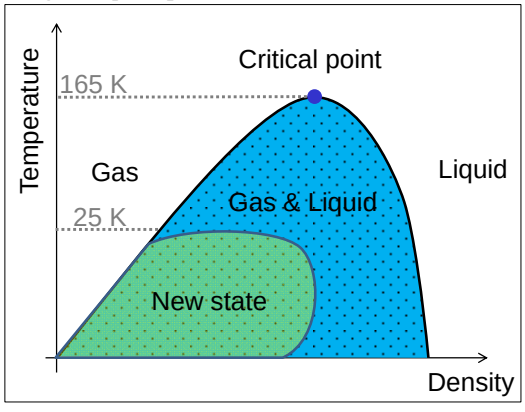

Fig. 1: Phase diagram of electrons and holes in diamond. Dotted area is occupied by the coexistent phase in equilibrium. A nonequilibrium continuous phase transition was found in the region labeled by "new state".

References

[1] J. S. Wang and C. Kittel, Phys. Lett. **42A**, 189 (1972).
[2] J. Omachi et al., Phys. Rev. Lett. **111**, 026402 (2013).
[3] R. Shimano et al., Phys. Rev. Lett. **88**, 057404 (2002).

Angular dependence of high-field low-temperature phase in a Pauli limited d-wave superconductor

Condensed matter theory group Kenichi Hosoya

Abstract We investigate the angular dependence of the high-field low-temperature (HFLT) phase in a heavy fermion superconductor $CeCoIn_5$ on the basis of a microscopic approach. We confirm the picture that, with increasing the tilt angle, both the antiferromagnetic (AFM) and Fulde-Ferrell-Larkin-Ovchinnikov (FFLO) orders are gradually suppressed, and that disappearance of the AFM order down to the zero-temperature limit occurs at a lower angle than that of the FFLO state.

Recently, the quasi-two-dimensional (Q2D) heavy-fermion superconductor $CeCoIn_5$ has attracted much attention due to a possible realization of a FFLO superconducting (SC) state in its high-field low-temperature (HFLT) SC phase [1]. On the other hand, neutron scattering measurements in $\mathbf{H} \perp c$ have revealed the existence of an incommensurate antiferromagnetic (AFM) order within the HFLT SC phase [2]. To try to understand the origin of this AFM order, several mechanisms have been proposed. We have proposed that AFM order is induced by the d-wave pairing symmetry and a strong Pauli-paramagnetic pair-breaking (PPB) effect [3].

More recently, NMR data obtained by tilting the field direction from the a-b plane have revealed that with tilting the field from the a-b plane, the AFM ordered region is pushed down to lower fields and pure (nonmagnetic) FFLO phase appears just below H_{c2} [4].

In this study, we discuss the angular dependence of the HFLT phase. We confirm that the appearance of pure FFLO state observed in the NMR measurement is due to the incomplete nesting condition. In this calculation, we find that, with increasing the tilt angle, both the AFM and FFLO orders are gradually suppressed, and that disappearance of the AFM order in the zero-temperature limit occurs at a lower angle than that of the FFLO state. We also find that, in agreement with the observation [4], the AFM order in real space tends, as the field direction is tilted, to occur only close to the FFLO nodal planes [5].

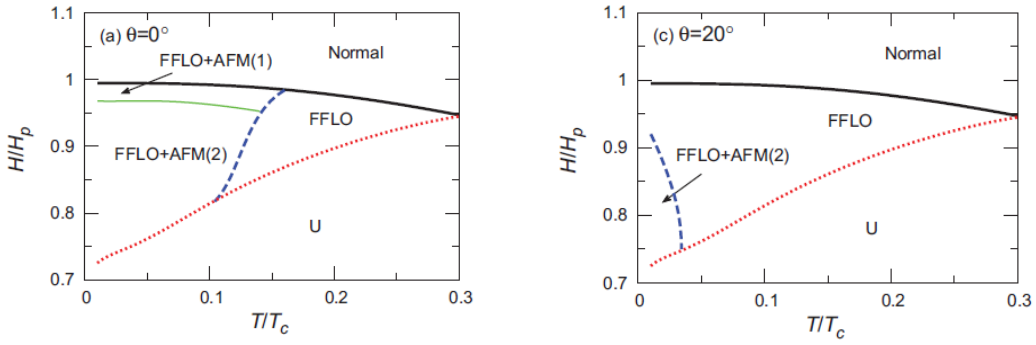

Fig. 1. H-T phase diagrams in the $\mathbf{H} \perp c$ case and at the rotated angle.

References

[1] H. Adachi and R. Ikeda, Phys. Rev. B 68, 184510 (2003).
[2] M. Kenzelman et. al., Science. 321, 1652 (2008) .
[3] Y. Hatakeyama and R. Ikeda, Phys. Rev. B 83, 224518 (2011).
[4] K. Kumagai, H. Shishido, T. Shibauchi, and Y. Matsuda, "Angle Dependence of Magnetic Order and the FFLO Phase of $CeCoIn_5$" preprint (unpublished).
[5] K. Hosoya and R. Ikeda, Phys. Rev. B 88, 094513 (2013).

Nonlinear spin dynamics induced by intense terahertz magnetic field

Solid State Spectroscopy Group Yu Mukai

Abstract Nonlinear spin dynamics in the antiferromagnet crystal has been investigated by time-resolved magneto-optical measurements with an intense terahertz magnetic field excitation. We found that the frequency of the antiferromagnetic resonance is red-shifted and the decay rate of the magnetization change is increased under the strong terahertz magnetic field.

Nonlinear dynamics of many-body spin systems has been an important research field and attracted considerable attention from the perspective of fundamental physics and technological applications. Recently a considerable research interest has been focused on spin dynamics of antiferromagnet whose magnetic response takes place in the terahertz (THz) frequency region due to a large exchange interaction between spins. THz magnetic field resonant to the antiferromagnetic mode is the most advantageous for the direct magnetic excitation suppressing undesirable thermal effects [1]. However, no observation of the nonlinear feature of the THz magnetic response, so far, has been reported due to the lack of sufficient intense THz light sources. It is necessary to explore more efficient excitation method to drive the antiferromagnetic spin system into the nonlinear regime. In this study we have established a novel THz magnetic excitation method based on the field enhancement with the split ring resonator (SRR) [2], and have clarified the nonlinear feature of antiferromagnetic spin dynamics by using this magnetic excitation method. The SRRs array was deposited on the $HoFeO_3$ crystal surface to generate the strong THz magnetic field. We measured time-development of the local magnetization change induced by strong THz pulse excitation in the vicinity of the SRR by using the time-resolved magneto-optical (MO) microscopy.

Figure 1(a) shows the observed MO signal corresponding to the magnetization change associated with an antiferromagnetic resonance. We applied the analytic signal approach to obtain the instantaneous frequency and envelope amplitudes to elucidate the dynamical feature of the signal. Figure 1 (b) shows the time-responses of the instantaneous frequency obtained from temporal waveforms at different excitation intensities. One can see clearly large frequency shift occurs at the high intensity case. The redshift of the antiferromagnetic resonance of $HoFeO_3$ depends on the amplitude of the magnetization oscillation. This result provides a direct proof of the nonlinearity in the collective motion of the antiferromagnetic spins. In addition, we found that the decay process of the magnetization change has strong excitation intensity dependence. As shown in the Fig. 1(c), the decay time of the magnetization amplitude becomes short for the high intensity excitation. This suggests that a nonlinear spin relaxation process should take place in the strongly driven regime.

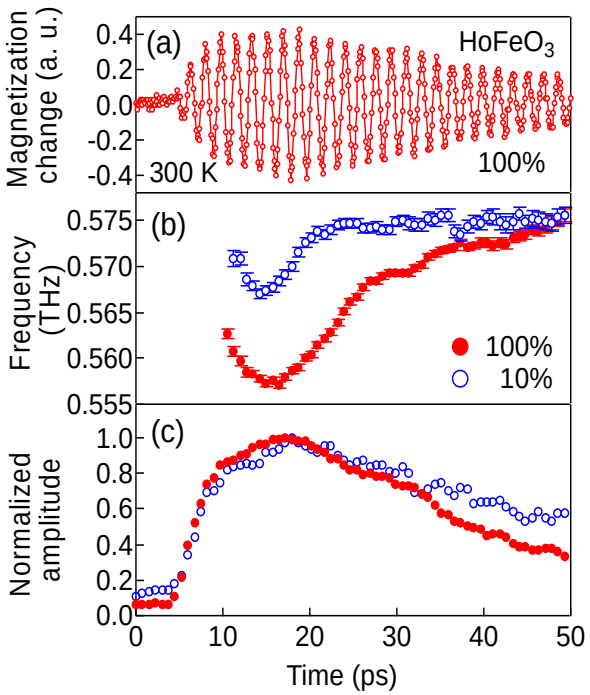

Fig. 1: (a) Time response of the magnetization change on the $HoFeO_3$ crystal surface induced by THz magnetic field. (b) Instantaneous frequency and (c) envelope amplitudes for the different excitation intensities.

References

[1] T. Kampfrath *et al*., Nature Photon. **7**, 680 (2013).

[2] Y. Mukai *et al*., Appl. Phys. Lett. **105**, 022410 (2014).

Classifying neuronal spike trains as analog or digital coding

Nonlinear dynamics group, Yasuhiro Mochizuki

Abstract Sensation and motion are represented and processed in the brain as series of neuronal discharges called spikes or firings. Here we classify *in vivo* spike trains either as analog or digital coding, and compare information representation strategy among different brain regions.

Animal's behavior is operated by neuronal spikes in the brain. A central issue of neural coding is to discern the manner in which the sensory information is represented and processed, and finally transformed into motion, all in terms of neuronal spikes.

Assuming that neural systems have evolved to optimize their efficiency in information transmission and processing, it is expected that individual areas of the brain process signals in different ways depending on their functions. For instance, the elaborate control of motion may require delivering continuous values. In such a case, it is expected that continuous values are transmitted in terms of the neuronal firing rates [1]. On the contrary, there may be other kinds of computation that needs to transmit and process discrete signals as in decision processes. Such information processing can be manifested by jumping among quasistationary attractor states of neural networks represented as sets of distinct firing rates [2,3]. It has also been shown theoretically that the structure of the tuning curve that achieves the optimal information transmission rate can be either continuous or discrete depending on the length of the coding window [4,5]. Therefore, some brain regions may transmit continuous values by modulating continuous firing rates, whereas other regions may process information in terms of discrete values by switching discrete firing rates.

Here we suggest classifying spike trains according to whether the underlying firing rate of a spike train is likely to be continuously varying or switching between active and inactive states [6]. In this contribution, we apply this method to *in vivo* spike trains, and report the results of the analysis.

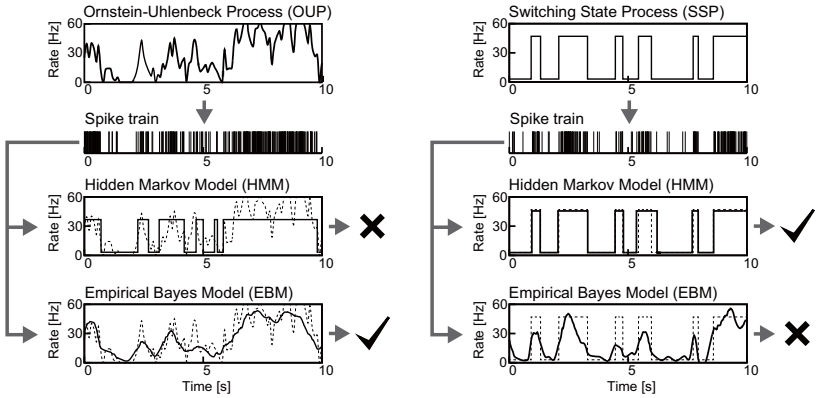

Fig. 1. Analog-digital classification of neuronal spike trains.

References

[1] A. P. Georgopoulos *et al.*, J. Neurosci., **2**, 1527-1537 (1982).

[2] D. J. Amit, *"Modeling Brain Function: The World of Attractor Neural Networks"*, (Cambridge University Press, Cambridge, 1989).

[3] M. Abeles *et al.*, Natl. Acad. Sci. USA, **92**, 8616-8620 (1995).

[4] M. Bethge *et al.*, Phys. Rev. Lett., **90**, 088104 (2003).

[5] A. Nikitin *et al.*, Phys. Rev. Lett., **103**,138101 (2009).

[6] Y. Mochizuki and S. Shinomoto, Phys. Rev. E, **89**, 022705 (2014).

Quantum Gas Microscope of Two-electron Atoms – high-resolution imaging of ultracold ytterbium atoms in a 2D optical lattice –

Quantum Optics Group Ryuta Yamamoto

Abstract We develop an ytterbium (Yb) quantum gas microscope (QGM). We successfully detect single ^{174}Yb atoms in a two-dimensional optical lattice. The achieved resolution of 212nm is less than the lattice constant of 266nm. This result opens up various possibilities of a QGM using fermionic and/or bosonic Yb atoms.

Ultracold atom system in an optical lattice is a quite useful platform for studying the condensed matter physics. In recent studies, it is reported that a single atom in an optical lattice is observed with a high-resolution imaging system [1,2]. This detection method is called a "Quantum Gas Microscope (QGM)", by which we can directly observe local properties and quantum dynamics with a single site resolution in an optical lattice [2,3,4]. In spite of its great importance, a QGM is realized only for a bosonic rubidium (Rb) atom. From the viewpoint of quantum simulation of condensed matter system, it is strongly desired to realize a QGM of a fermionic atom.

In this work, we successfully develop a QGM using an ytterbium (Yb) atom, which is an alkaline-earth like atom and has many stable isotopes of 5 bosons and 2 fermions. We have already reported that we succeeded in cooling and detecting a bosonic isotope of ^{174}Yb in a two-dimensional (2D) optical lattice with "dual molasses" technique in which we use two kinds of molasses beams; one is used as a probe ("blue molasses") and another one is used as a cooling ("green molasses") [5]. Quite recently we improve the imaging system, such as the focus positon and the tilt of objective lens, for achieving a higher resolution. We also enhance the cooling efficiency of "dual molasses" by applying a sideband cooling [6] in addition to the Doppler cooling. As a result we succeed in keeping the fluorescence in a quite long time and almost successfully freeze atoms in the same lattice site. Moreover, we combine the improved system with the high resolution spectroscopy of the ultranarrow optical transition between the ground $^1S_0$ state and the metastable $^3P_2$ state. As a result, we successfully prepare several tens of atoms and detect only a few isolated atoms in a 2D optical lattice with high sensitivity, as shown in Fig. 1(a). We average over fluorescence signals of 10 single isolated atoms and the resolution of average image is 212(4) nm, which is 1.89(3) times of the ideal resolution, as shown in Fig.1 (b).

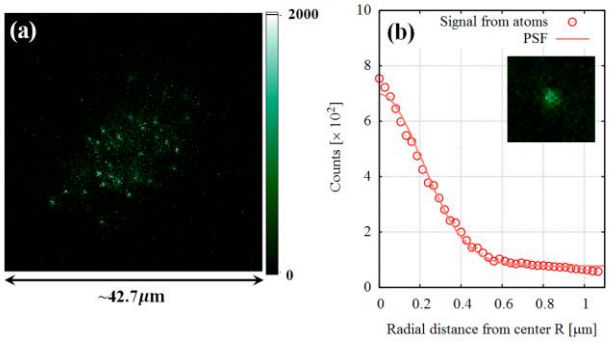

Fig. 1. (a) Fluorescence image of dilute cloud of atoms in a 2D optical lattice. (b) The fluorescence distribution of single isolated atom by averaging over 10 single atoms. The line is a fit with the Gaussian. It shows the resolution σ ($1/e^{1/2}$ half-length) of imaging system is 212(4) nm, which is 1.89(3) times of the ideal resolution.

Further tuning of experimental conditions of our QGM will enable us to perform many interesting quantum simulation studies using Yb atoms.

References

[1] W. S. Bakr *et al.* Nature **462**, 5 (2009)
[2] J. F. Sherson *et al.*, Nature **467**, 68 (2010).
[3] W. S. Bakr *et al.*, Science **329**, 547 (2010).
[4] T. Fukuhara *et al.*, Nature Physics **9**, 235-241 (2013).
[5] K. Shibata *et al.*, J. Phys. Soc. Jpn. **83**, 014301 (2013).
[6] D. J. Wineland *et al.*, Phys. Rev. A **20**, 1521 (1979).